Supporting Information

1. **SI Materials and Methods**
2. **Table S1. Data collection and refinement statistics**
3. **Figure captions**
4. **Figure S1-S10**

SI Materials and Methods

Cloning

Polymerase chain reactions (PCR) were performed using *PfuUltra*^{TM} high-fidelity DNA polymerase (Stratagene) to clone the full-length ISAV-M1 (aa 1-196), M1-N (aa 1-119) and M1-C (aa 120-196). Our ISAV-M1 sequence was originally cloned from the Maine 2003 isolate, but its nucleic acid sequence is identical to the one from the Canadian CA/NS/G0008/2012 isolate deposited at the GenBank (ANM86266.1). PCR products were digested with NdeI and XhoI (New England Biolabs) at 37°C for 4 hours. The digested PCR products for the full-length M1 and M1-N were inserted into the pET28b+ vector, whereas the digested PCR product of M1-C was cloned into the pETDeut-1 vector with 6xHis and SUMO at the N-terminus. A 6xHis fusion tag was added to the N-terminus of both M1 and M1-N to facilitate protein purification. The M1-C should have two extra residues H and M at its N-terminus after the His-tagged SUMO domain was removed by the SUMO protease.

Two M1 mutants named M1-4KA and M1-3KA, each containing the mutations K30A/K31A/K32A/K33A and K63A/K66A/K68A, respectively, were generated by PCR using the pET28b+ harboring the full-length ISAV-M1 coding sequence as template. All identified clones were transformed into Rosetta 2 *E. coli* cells (DE3) (Novagen) for protein expression.

Expression, purification, and crystallization

The expression of M1 proteins was induced with 1 mM IPTG at 15°C for 24 hours after the cell density had reached an OD_{600nm} of 0.6. Cells were collected and sonicated in a lysis buffer containing 300 mM NaCl, 5 mM Imidazole, 10% (v/v) glycerol, and 50 mM Tris-HCl at pH 7.5. The lysate was centrifuged at 40,000×g for 30 min, and the supernatant was used for further purification. Full-length M1, M1-N and the two mutants M1-4KA and M1-3KA were purified sequentially using a HisTrap^{TM} HP Column (GE Healthcare) and a Superdex^{TM} 200 Column (GE Healthcare). For the M1-C protein, the sample was applied to the HisTrap^{TM} HP Column for a second time to remove the 6xHis-tagged SUMO domain after the treatment with SUMO protease overnight. Purified proteins were at least 95% pure according to Coomassie-stained SDS–polyacrylamide gels.

The best native M1 crystals were grown at 20°C for three days using the microbatch-under-oil crystallization method. Al's Oil (Hampton Research) was first poured into the trough area of the 72-Well Microbatch Plate (Hampton Research) so all 72 wells were submerged under oil. The crystallization drop, which was made of 3 µl of protein solution (20 mg/ml in 200 mM NaCl, 10% glycerol, and 25mM Tris-HCl at pH 7.5) and 1 µl of mother liquor (containing 0.2 M NaCl, 14% PEG 3350, and 0.1 M BIS-TRIS at pH 6.5), was briefly mixed and then pipetted into each well. To prepare the heavy atom derivative, native M1 crystals were soaked in mother liquor containing 5 mM gold(III) chloride overnight at room temperature. The crystals were then back-transferred to mother liquor without heavy atom. M1 crystals were cryo-protected using mother liquor containing 30% (v/v) glycerol.

Data collection and structure determination

The N-terminal His-tagged protein was used for structural determination because it consistently produced crystals with better diffraction. The diffraction data were collected from single crystals at the Life Sciences Collaborative Access Team (LS-CAT) beamline at the Advanced Photon Source (APS). All diffraction data were processed using HKL2000 (1). The structure was determined by single isomorphous replacement with anomalous scattering (SIRAS) (Table S1). AutoSHARP was used for heavy atom refinement and experimental phase calculation. The protein model was built with Autobuild (PHENIX) and also by hand with COOT (2). The structural model was refined using phenix.refine (3). Structure figures were produced using PyMOL unless otherwise specified (The PyMOL Molecular Graphics System, Version 1.2r3pre, Schrodinger, LLC). The coordinates of ISAV-M1 have been deposited in the Protein Data Bank (PDB ID 4Z7T).

Fluorescence polarization assays

5’-fluorescein-labeled and unlabeled RNA oligomers of simple AC repeats were purchased from Thermo Fisher Scientific and Sigma-Aldrich. For the binding affinity measurements, the binding solution contained 0.1 mM $MgCl_2$, 20 mM HEPES at pH 7.5, and 5 nM fluoresceinated RNA. This solution should also contain approximately 10 mM NaCl generated during pH adjustment as HCl was titrated to the HEPES sodium salt. M1 samples

were titrated into the binding solution until the millipolarization (mP) reading stabilized. Experiments were carried out at 20 °C. Each protein titration was repeated in triplicate. The RNA binding data were analyzed using the equation $P = \{(P_{bound} - P_{free})[protein]/(K_d + [protein])\} + P_{free}$, where P is the polarization measured at a given total protein concentration, P_{free} is the initial polarization of fluorescein-labeled RNA without protein bound, P_{bound} is the maximum polarization of RNA when all are bound by protein, and [protein] is the protein concentration. The free and total protein concentrations were assumed to be equal since the K_d was at least 10-fold higher than the concentration of fluorescein-labeled RNA. A total of three parameters, including P_{bound}, P_{free} and K_d, were fitted by nonlinear least-squares regression analysis.

For the binding stoichiometry measurements, the assay conditions were identical to those used for the affinity determination, except that the total RNA concentration was increased to 1 μM by adding corresponding unlabeled RNA. The data were analyzed as described (4).

Co-migration assay

To detect the interaction between ISAV M1 and NP, gel filtration experiments were carried out using a Superdex^{TM} 200 Column in the buffer containing 200 mM NaCl, 10% glycerol, and 25 mM Tris·HCl pH 7.5. Purified M1 and NP proteins (4) were mixed at a 2:1 ratio and incubated for 2 hours at 4°C before injected into the column. To test the effect of RNA on M1-NP interaction, M1, NP and a 24-nt RNA were mixed together at a 2:1:1/10 ratio. Eluted fractions were applied to SDS–polyacrylamide gels and visualized by Coomassie-staining.

Cryo electron tomography of the ISA virion

Cells and virus: The Atlantic Salmon Kidney (ASK) cells (CRL-2747, ATCC) from Atlantic salmon (*Salmo-salar*) was grown in Leibovitz's L-15 Medium (ATCC, 30-2008) supplemented with 10% fetal bovine serum (FBS; ATCC, 30-2020), 4 mM L-glutamine and 50 μg/ml penicillin-streptomycin at 20 °C. A strain of infectious salmon anemia (ISAV), isolated from infected Atlantic salmon in Maine 2003, was used to infect ASK cells.

Virus purification: ISAV was propagated by multiple passages on confluent monolayers of ASK cells, as described (5). Briefly, ASK cells grown in 150-cm^2 flasks at 20 °C were inoculated with ISAV at a multiplicity of infection of 1.0 for 3-4 hours. Then, L-15 medium and 5% FBS was added and the flasks were incubated at 15 °C until extensive cytopathic effect (CPE) was observed. The supernatant was harvested 12-14 days post-infection and clarified by low-speed centrifugation at 5,000 x g for 30 min at 4°C. Crude ISAV present in the supernatant (obtained from ninety 150-cm^2 flasks) was precipitated by the addition of 70 g polyetheylene glycol 8000, and 23.2 g of NaCl per liter, and stirring the suspension overnight at 4°C. The precipitate was collected by centrifugation at 17,000 x g for 90 min (Sorvall, GSA rotor) and suspended in 34 ml of TNE (0.1 M Tris-HCl, pH7.3, 0.1 M NaCl, 1mM EDTA) buffer. The suspension (17 ml per tube) was layered onto a cushion of 56% (7.0 ml) to 28% (15.0 ml) sucrose gradient and centrifuged at 120,000 x g for 2 hours at 4°C (Beckman, SW28 rotor). An opaque virus band at the 28-56% interphase was collected using a wide bore P1000 pipette. Sucrose was removed by centrifuging the concentrated virus solution (8.0 ml) using a 10K cut-off filter (Millipore), and the purified virus (1.5 ml; concentration 2.664 mg/ml) was stored at 4°C until use.

Electron microscopy: Freshly prepared virus samples were mixed with 10 nm fiducial gold markers and deposited onto holey carbon grids. Grids were briefly blotted with filter paper and plunge frozen in liquid ethane. The grids were imaged at -170 °C on a 300kv Technai F30 Polara (FEI) equipped with a K2 Summit direct electron detector (Gatan). Tilt series were collected in dose fractionation mode at a magnification of 15,500x, resulting in a final pixel size of 2.6 Å. Using SerialEM (6), low-dose, single-axis tilt series were collected at -6 defocus with a cumulative dose of ~60 e/$Å^2$ distributed over 41 images and covering an angular range of -60° to +60°, with angular increments of 3°. Tilt series were aligned and reconstructed using IMOD (7). In total, 10 tomographic reconstructions were generated by using Weighted Back Projection (WBP) and used for further processing. UCSF chimera (8) was used for 3D surface rendering of the subtomogram averages. The crystal structure of ISAV M1 protein was docked into M1 layer in the electron microscope structure using the "fit in map" function in UCSF chimera.

Liposome association assays

Pre-formed liposomes of different POPC (1-palmitoyl-2-oleyl-sn-glycero-3-phosphocholine) and DOPS (1,2-dioleyl-sn-glycero- 3-phospho-L-serine) (Avanti Polar Lipids) composition and trace amounts of ^{3}H-1-palmitoyl 2-palmitoylphosphatidylethanolamine (DPPE) (American Radiolabeled Chemicals) were made by extrusion. Lipid mixes in chloroform were dried under a nitrogen stream and then resuspended in a Tris buffer (25 mM Tris-HCl pH7.5, 200 mM NaCl, 10% glycerol, 5 mM β-Mercaptoethanol) to a final lipid concentration of 10mM. Large unilamellar vesicles (LUVs) were made by 10 freeze-thaw cycles in liquid nitrogen. LUVs were then passed through a polycarbonate membrane with 50, 100, or 400 nm pore size (Avanti Polar Lipids). Liposome lipid concentration was measured by scintillation counting.

Liposome association was assayed using a discontinuous Accudenz gradient following previously described protocol with the following modifications (9). Liposomes (1 mM lipid concentration) were incubated with M1 protein at a 200 Lipid:Protein molar ratio in the Tris buffer overnight. After incubation, 150 µl of the protein/liposome mixture was added to 150 µl 80% (w/v) Nycodenz in the Tris buffer, bringing it to a 40% (w/v) Nycodenz solution. The mixture was placed in a 5x41 mm Ultra-Clear tube (Beckman) and overlaid with 250 µl 30% (w/v) Nycodenz in the Tris buffer and then with 50 µl Tris buffer without glycerol. The gradient was centrifuged in a Sw-55 Ti rotor for 4 hrs at 48,000 rpm and 4 ^{o}C. The three layers were collected and samples were run on an SDS-PAGE and Coomassie stained. Percent of protein recovered from each layer was calculated by gel band intensity analysis using the ImageJ software.

References

1. Otwinowski Z, Minor W, & et al. (1997) Processing of X-ray diffraction data collected in oscillation mode. *Methods Enzymol* 276:307-326.
2. Emsley P & Cowtan K (2004) Coot: model-building tools for molecular graphics. *Acta Crystallogr D Biol Crystallogr* 60(Pt 12 Pt 1):2126-2132.
3. Adams PD*, et al.* (2010) PHENIX: a comprehensive Python-based system for macromolecular structure solution. *Acta Crystallogr D Biol Crystallogr* 66(Pt 2):213-221.
4. Zheng W, Olson J, Vakharia V, & Tao YJ (2013) The crystal structure and RNA-binding of an orthomyxovirus nucleoprotein. *PLoS Pathog* 9(9):e1003624.
5. Falk K, Namork E, Rimstad E, Mjaaland S, & Dannevig BH (1997) Characterization of infectious salmon anemia virus, an orthomyxo-like virus isolated from Atlantic salmon (Salmo salar L.). *J Virol* 71(12):9016-9023.
6. Mastronarde DN (2005) Automated electron microscope tomography using robust prediction of specimen movements. *J Struct Biol* 152(1):36-51.
7. Kremer JR, Mastronarde DN, & McIntosh JR (1996) Computer visualization of three-dimensional image data using IMOD. *J Struct Biol* 116(1):71-76.
8. Pettersen EF*, et al.* (2004) UCSF Chimera--a visualization system for exploratory research and analysis. *J Comput Chem* 25(13):1605-1612.
9. Scott BL*, et al.* (2003) Liposome fusion assay to monitor intracellular membrane fusion machines. *Methods Enzymol* 372:274-300.

Table S1. Data collection and refinement statistics

	Native	$AuCl_3$ derivative
Data collection		
Wavelength (Å)	0.97856	0.97872
Space group	$P2_1$	$P2_1$
Unit-cell dimensions		
a,b, c (Å)	38.8, 95.9, 85.4	38.6, 95.9, 85.8
β(°)	93.0	92.7
Resolution, Å	50-2.6 (2.64-2.6)	50-3.25 (3.31-3.25)
R_{merge}, %	9.1 (82.5)	14.4 (43.8)
I/σ	15.89 (2.05)	17.13 (7.61)
Completeness, %	98.5 (98.2)	100 (100)
Redundancy	4.7 (4.0)	7.6 (7.7)
Phasing		
No. of sites	-	5
FOM	-	0.26
Refinement		
Resolution (Å)	47.95 – 2.6	
R_{work} / R_{free} (%)	19.2 / 25.8	
No. of R_{free} set (%)	949out of 17918, 5.0%	
Average B factor ($Å^2$)	67.04	
R.m.s. deviations		
Bond lengths(Å)	0.011	
Bond angles (°)	1.674	
Ramachandran		
Favoured	547, 93%	
Allowed	38 , 6.5%	
Outliers	3 , 0.5%	

The numbers in parentheses are for the highest-resolution shell.

Figure Legends

Figure S1. Gel filtration chromatograms. The eluted positions of free ISAV-M1 and NP are marked by arrows. Fraction numbers are marked on the horizontal axis. The elution curves of four samples are shown, including M1 (red), NP (pink), M1+NP (blue), and M1+NP+RNA (cyan). Two SDS-PAGE gels are shown on the left to detect any complex formation for the M1+NP and M1+NP+RNA samples. Lane M, marker; lane IN, Input; lanes 32-49, different eluted fractions. Molecular weights for the various marker bands are indicated. Protein bands corresponding to M1 and NP are marked on the right.

Figure S2. The two cysteines (i.e. C13 and C115) near the linker loop assume different structural conformations in the three ISAV-M1 molecules. Molecules A, B, and C related by the pseudo translation symmetry are colored in green, magenta and yellow, respectively. Two cysteines (i.e. C13 and C115) in each molecule are shown by red sticks. C13 and C115 form a disulfide bond in the molecule C but not in molecules A and B.

Figure S3. Phylogenetic trees of M1 proteins from orthomyxoviruses. Representative sequences of the M1 proteins of Influenza A virus, Influenza B virus, Influenza C virus, Influenza D virus, Thogoto virus and Isa virus were analyzed. The M1 protein from the ISAV isolate Maine 2003 used in this study is highlighted with a black dot.

Figure S4. Conservation of M1 proteins across different genera within the *Orthomyxoviridae* family. The bottom-left section shows structure-based comparison by Dali while the up-right section shows sequence-based comparison by ClustalW. Protein sequence ID's and PDB ID's are provided in the top row and left column, respectively. FluB and FluD M1 protein structures are not yet available and therefore left out for structural comparison.

Figure S5. Buried surface areas between adjacent ISAV-M1 molecules in the 2-D crystal lattice. The schematic drawing is the same as in Figure 2C. The buried surface areas and the corresponding interface between B2 and each of the eight surrounding molecules are shown in the table.

Figure S6. Close-up views of the intermolecular interactions mediating the formation of the

2-D lattice. The schematic drawing is the same as in Figure 2C. The reference molecule B2 is shown in white.

Figure S7. Alignment of M1 protein sequences from 11 ISAV isolates. Maine 2003 is the isolate used in this study. Only unique M1 sequences are included. Isolates having identical M1 sequences as those shown in the figure were excluded from the alignment. Several M1 sequences are incomplete with missing residues represented by dashes. CLUSTALW was used to align the amino acid sequences. The residues important for M1 lattice formation, including H10, E16, Q72, N75, S79, S94, Q155, A158, S163, A172, M189, Y194 (the same as shown in Figure S6), are highlighted in yellow.

Figure S8. Two clusters of positively charged surface residues in the M1-N domain. One cluster, consisting of K30, K31, K32, and K33, is located between α3 and α4. The other cluster containing K63, K66 and K68 is located between α5 and α6. (A, C) Surface representation of ISAV-M1 colored by electrostatic potential view from two different directions. (B, D) Ribbon diagram of ISAV-M1 colored in rainbow viewed from the same direction as in (A, C). Charged residues are shown by magenta sticks.

Figure S9. K63, K66 and K68 mapped onto the ISAV-M1 2-D lattice. A 3x3 array is shown. Molecules are colored by electrostatic potential, and a single repeating unit is highlighted. The three lysine residues are fully exposed on the top face of the lattice.

Figure S10. ISAV-M1 RNA binding. (A) RNA binding affinity measurements for the full length M1. FA was performed using three ssRNA oligos each containing 12, 24, and 48nts. (B) RNA binding stoichiometry measurements for the full length M1 using a 24-nt ssRNA oligo. (C) RNA binding affinity measurements for the ISAV-M1-N and ISAV-M1-C. (D) RNA binding affinity measurements for the ISAV-M1-3KA and M1-4KA mutants. The 24-nt long ssRNA oligo was used above unless otherwise mentioned.

Figure S1

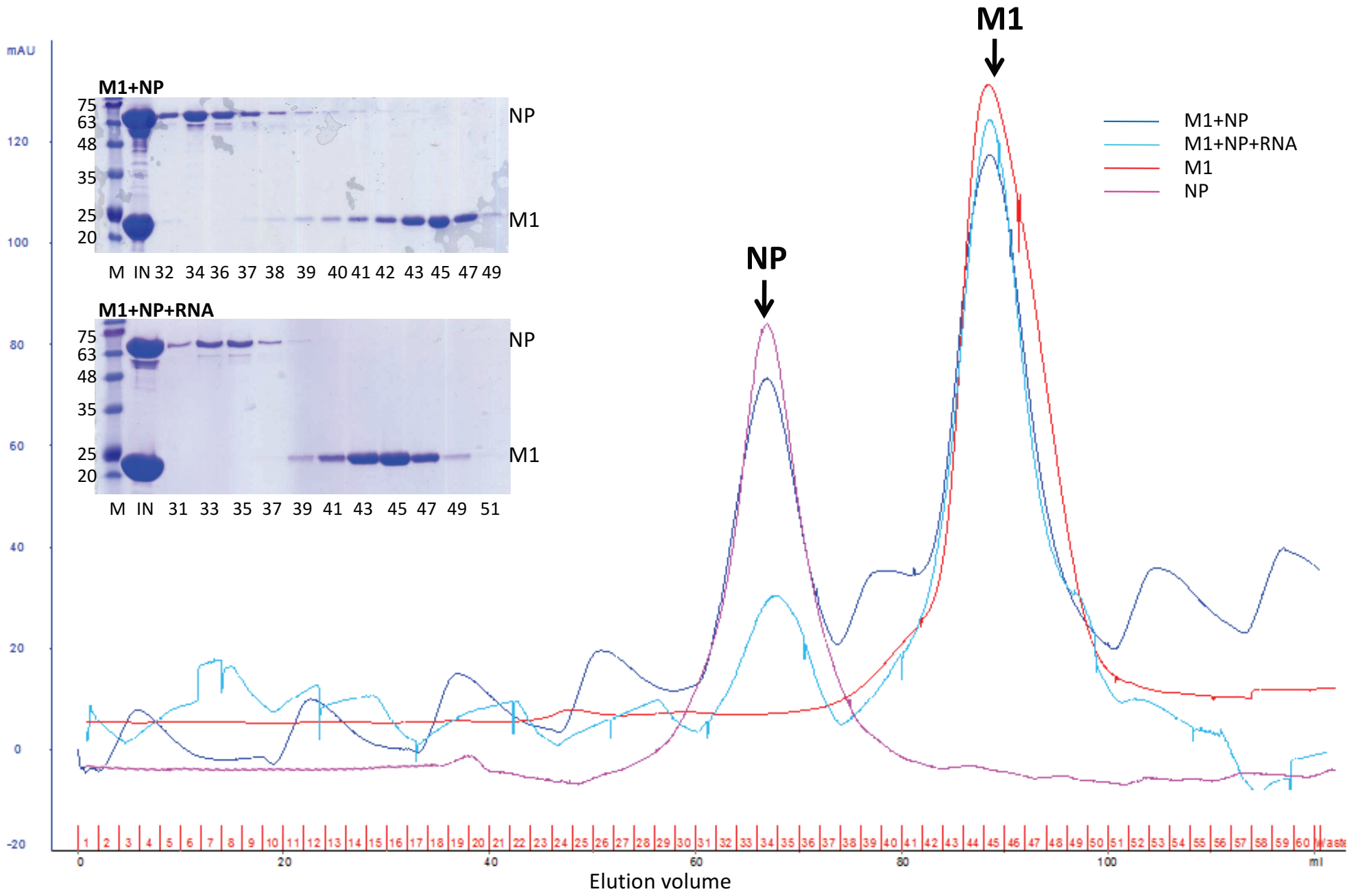
M1
NP
M1+NP
M1+NP+RNA
M1
NP
mAU
120
100
80
60
40
20
0
-20
0
20
40
60
80
100
ml
Elution volume
M1+NP
75
63
48
35
25
20
NP
M1
M IN 32 34 36 37 38 39 40 41 42 43 45 47 49
M1+NP+RNA
75
63
48
35
25
20
NP
M1
M IN 31 33 35 37 39 41 43 45 47 49 51

Figure S2

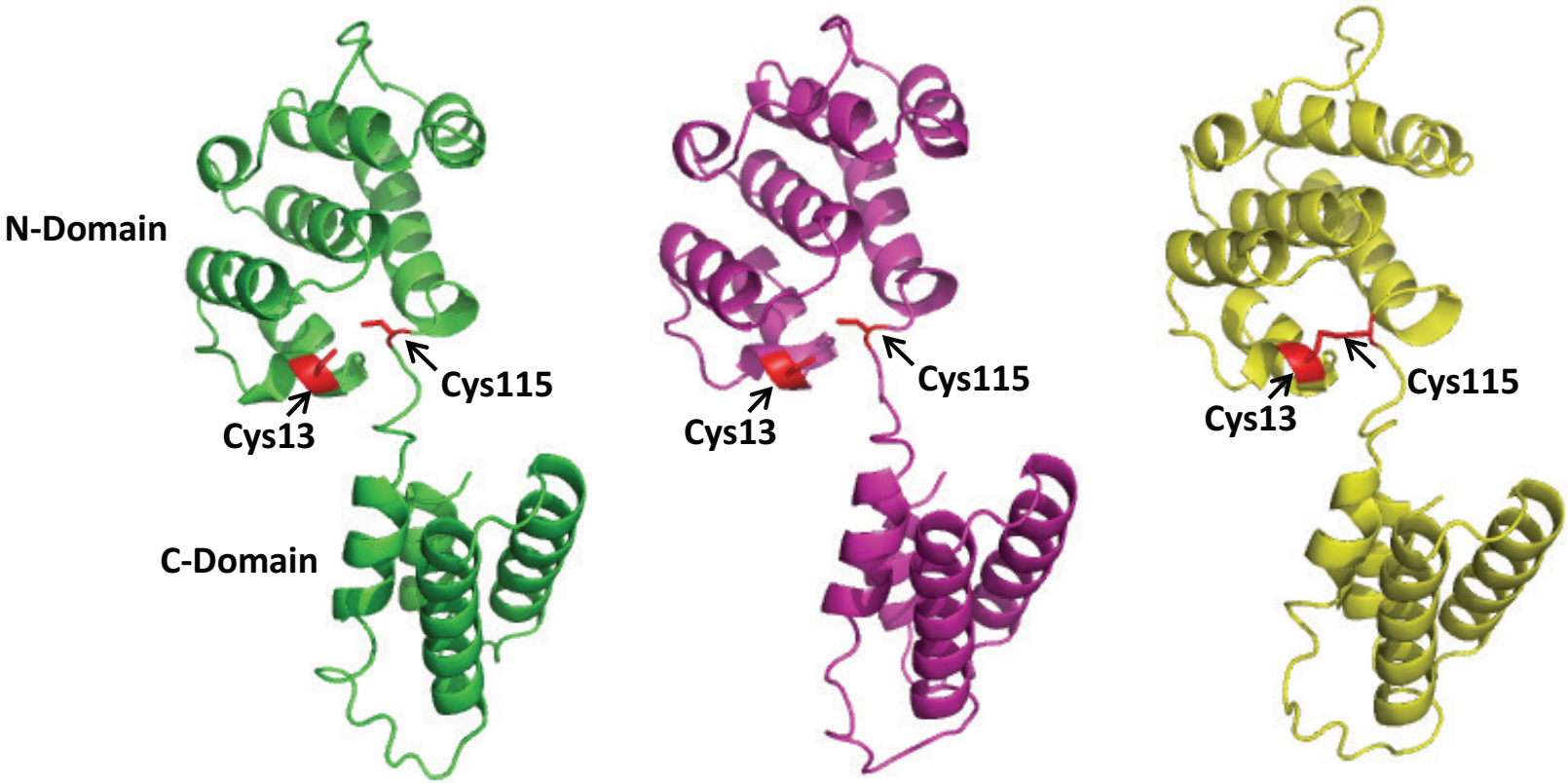
N-Domain
Cys115
Cys13
C-Domain
Cys115
Cys13
Cys115
Cys13
Molecule A
Molecule B
Molecule C

Figure S3

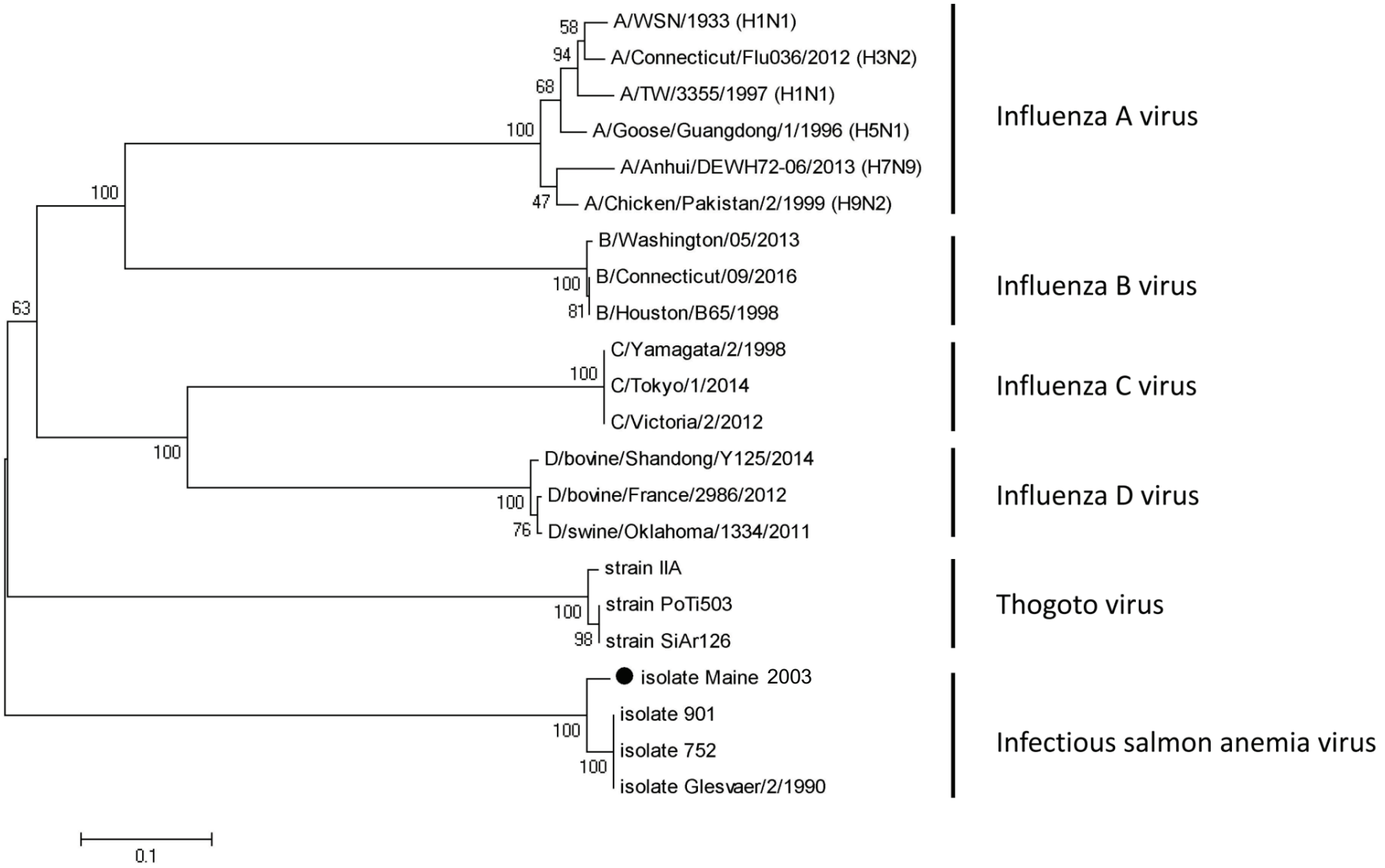
A/WSN/1933 (H1N1)
A/Connecticut/Flu036/2012 (H3N2)
A/TW/3355/1997 (H1N1)
A/Goose/Guangdong/1/1996 (H5N1)
A/Anhui/DEWH72-06/2013 (H7N9)
A/Chicken/Pakistan/2/1999 (H9N2)
B/Washington/05/2013
B/Connecticut/09/2016
B/Houston/B65/1998
C/Yamagata/2/1998
C/Tokyo/1/2014
C/Victoria/2/2012
D/bovine/Shandong/Y125/2014
D/bovine/France/2986/2012
D/swine/Oklahoma/1334/2011
strain IIA
strain PoTi503
strain SiAr126
isolate Maine 2003
isolate 901
isolate 752
isolate Glesvaer/2/1990
58
94
68
100
100
47
63
100
81
100
100
100
76
100
100
98
100
100
0.1
Influenza A virus
Influenza B virus
Influenza C virus
Influenza D virus
Thogoto virus
Infectious salmon anemia virus

Figure S4

	FluA (P03485)	FLuB (Q0PLR1)	FluC (Q6I7B9)	FluD (A0A088SJQ8)	Thogoto (Q80A33)	ISAV (Q910W0)
FluA (1EA3)		~29%	~12%	~16%	~10%	~11%
FLuB	–		~13%	~17%	~11%	~10%
FLuC (5M1M)	14.8	–		~42%	~12%	~12%
FluD	–	–	–		<10%	~16%
Thogoto (5I5O)	9.2	–	9.0	–		~12%
ISAV	4.1	–	4.0	–	5.2	

Pairwise sequence alignment by ClustalW (% identity)

Pairwise structural alignment by Dali (Z score)

Figure S5

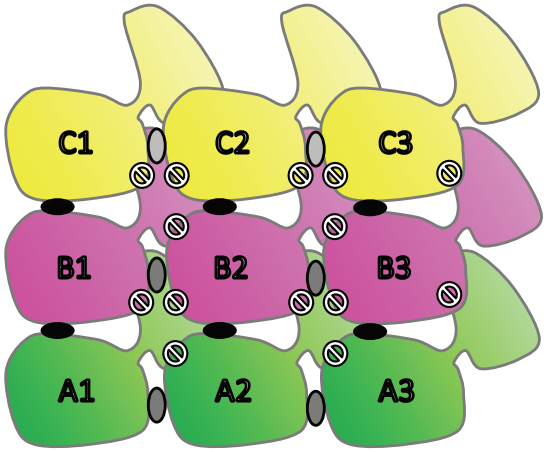

Molecule pairs	Buried surface (Å²)	Interface location	
B2-C2	2304	B2 N&C-domain	C2 N-domain
B2-A2	1639	B2 N-domain	A2 N&C-domain
B2-C3	858	B2 C-domain	C3 N-domain
B2-A1	433	B2 N-domain	A1 C-domain
B2-B1	286	B2 N-domain	B1 N-domain
B2-B3	286	B2 N-domain	B3 N-domain
B2-A3	6	–	–
B2-C1	0	–	–

Figure S6

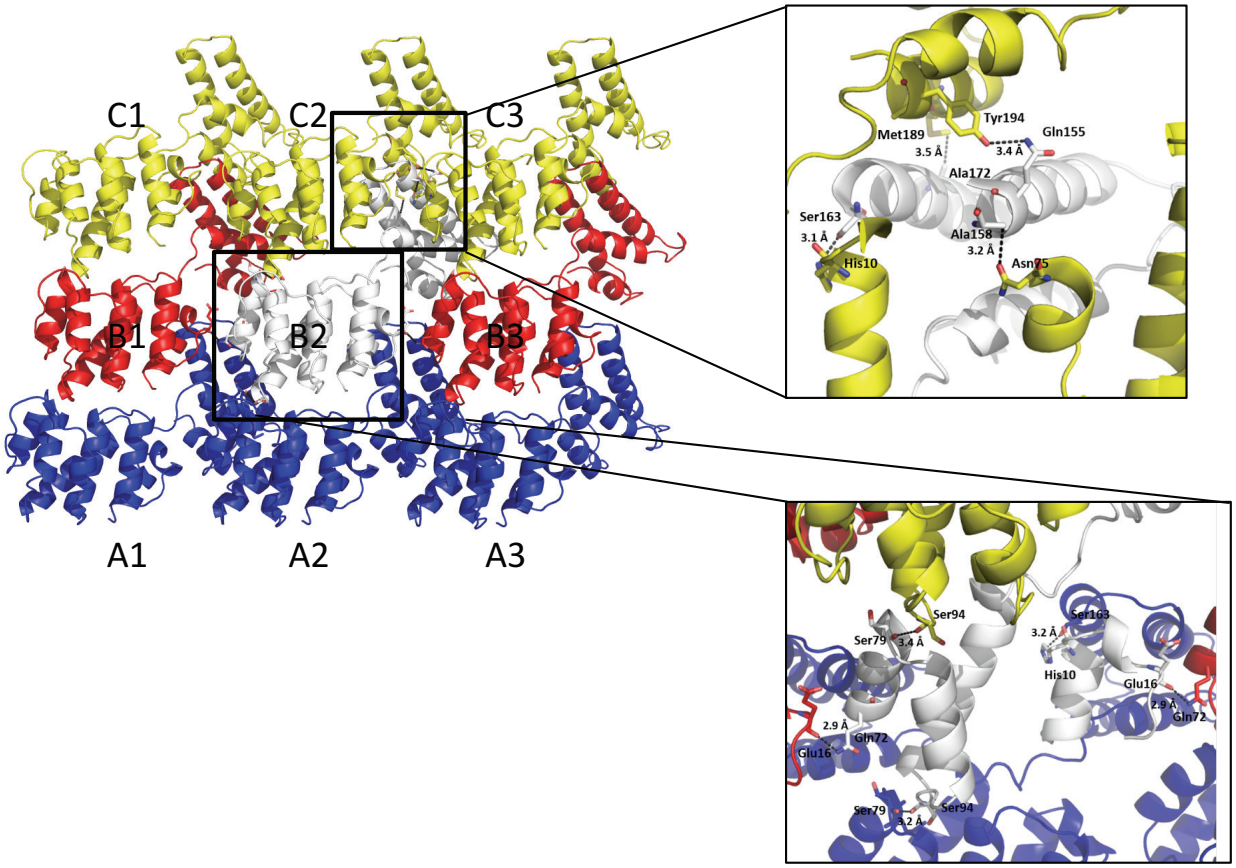
C1
C2
C3
B1
B2
B3
A1
A2
A3
Tyr194
Met189
Gln155
3.5 Å
3.4 Å
Ala172
Ser163
3.1 Å
Ala158
3.2 Å
His10
Asn75
Ser94
Ser79
3.4 Å
Ser163
3.2 Å
His10
Glu16
2.9 Å
Gln72
2.9 Å
Gln72
Glu16
Ser79
Ser94
3.2 Å

Figure S7


Maine 2003 1 MNESQWIQKHLPCMREANPKPRELIRHALKKKKRPEVVYAMGVLLTLGGESGLTVEFPVPEGKTVKVKTLNQLVNGMISRATMTLYCVMKDPPSGSMATL
CCBB 14 ----------MREANPKPRELIRHALKKKKRPEVVYAMGVLLTLGGESGLTVEFPVPEGKTVKVKTLNQLVNGMISRATMTLYCVMKDPPSGGMATL
U27573 1 MNESQWIQKHLPCMREANPKPRELIRHALKKKKRPEVVYAMGVLLTLGGESGLTVEFPVPEGKTVKVKTLNQLVNGMISRATMTLYCVMNDPPSGSMATL
CA/NS/2012-21/2012 1 MNESQWIQKHLPCMREANPKPRELIRHALKKKKRPEVVYAMGVLLTLGGESGLTVEVPVPEGKTVKVKTLNQLVNGMISRATMTLYCVMKDPPSGSMATL
CA/NB/G0047/2013 1 MNESQWIQKHLPCMREANPKPRELIRHALKKKKRPEVVYAMGVLLTLGGESGLTVEFPVPEGKTMKVKTLNQLVNGMISRATMTLYCVMKDPPSGSMATL
MT/Maine-2000 1 MNESQWIQKHLPCMREANPKPRELIRHALKKKKRPEVVYAMGVLLTLGGESGLTVEFPVPEGKTVKVKTLNQLVNGMISRATMTLYCVMKDPPSGSMATL
RPC/NB 02-1179-4 1 MNESQWIQKHLPCMREANPKPRELIRHALKKKKRPEVVYAMGVLLTLGGESGLTVEFPVPEGKTVKVKTLNQLVNGMISRATMTLYCVMKDPPSGSMATL
7833-1 1 MNESQWIQKHLPCMREANPKPRELIRHALKKKKRPEVVYAMGVLLTLGGESGLTVEFPVPEGKTVKVKTLNQLVNGMISRATMTLYCVMKDPPSGSMATL
MT/Maine-2003 1 MNESQWIQKHLPCMREANPKPRELIRHALKVKKRPEVVYAMGVLLTLGGESGLCVEFQAPEGKMVKVKTLNQLVNGMISRATMTLYCVMKDPPSGSMATL
Brekke/98 13 ----------CMREANPKPRELIRHALKVKKRPEVVYAMGVLLTLGGESGLCVEFQAPEGKMVKVKTLNQLVNGMISRATMTLYCVMKDPPSGSMATL
ISAV5(96/09/768) 1 MNESQWIQKHLPCMREANPKPRELIRHALKAKKRPEVVYAMGVLLTLGGESGLCVEFQAPEGKMVKVKTLNQLVNGMISRATMTLYCVMKDPPSGSMATL
RPC/NB 04-085-1 1 MNESQWIQKHLPCMREANPKPRELIRHALKVKKRPEVVYAMGVLLTLGGESGLCVEFQAPEGKMVKVKTLNQLVNGMISRATMTLYCVMKDPPSGSMATL
ISAV8(97/09/615) 1 MNESQWIQKHLPCMREANPKPRELIRHALKVKKRPEVVYAMGVLLTLGGESGLCVEFHAPEGKMVKVKTLNQLVNGMISRATMTLYCVMKDPPSGSMATL
Glesvaer/2/90 1 MNESQWIQKHLPCMREANPKPRELIRHALKVKKRPEVVYAMGVLLTLGGESGLCVEFQAPEGKMVKVKTLNQLVNGMISRATMTLYCVMKDPPSGSMATL
901_09 1 MNESQWIQKHLPCMREANPKPRELIRHALKVKKRPEVVYAMGVLLTLGGESGLCVEFQAPEGKMVKVKTLNQLVNGMISRATMTLYCVMKDPPSGSMATL
Maine 2003 101 MRDHIRNWLKEESGCQDADGGEEKWAMVYGMISPDMAEEKTMLKELKTMLHSRMQMYALGASSKALENLEKAIVAAVHRLPASCSTEKMVLLGYLK
CCBB 101 MRDHIRNWLKEESGCQDADGGEEKWAMVYGMISPDMAEEKTMLKELKTMLHSRMQMYALGASSKALENLEKAIVAAVHRLPASCSTEKMVLLGYLK
U27573 101 MRDHIRNWLKEESGCQDADGGEEKWAMVYGMISPDMAEEKTMLKELKTMLHSRMQMYALGASSKALENLEKAIVAAVHRLPASCSTEKMVLLGYLK
CA/NS/2012-21/2012 101 MRDHIRNWLKEESGCQDADGGEEKWAMVYGMISPDMAEEKTMLKELKTMLHSRMQMYALGASSKALENLEKAIVAAVHRLPASCSTEKMVLLGYLK
CA/NB/G0047/2013 101 MRDHIRNWLKEESGCQDADGGEEKWAMVYGMISPDMAEEKTMLKELKTMLHSRMQMYALGASSKALENLEKAIVAAVHRLPASCSTEKMVLLGYLK
MT/Maine-2000 101 MRDHIRNWLKEESGCQDADGGEEKWAMVYGMISPDMAEEKTMLKELKTMLHSRMQMYAP----------
RPC/NB 02-1179-4 101 MRDHIRNWLKEESGCQDADGGEEKWAMVYGMISPDMAEEKTMLKELKTMLRSRMQMYALGASSKALENLEKAIVAAVHRLPASCSTEKMVLLGYLK
7833-1 101 MRDHIRNWLKEESGCQDADGGEEKWAMVYGMISPDMAEEKTMLKELKTMLHSRMQMYALGASSKALENLEKAIVAAAHRLPASCSTEKMVLLGYLK
MT/Maine-2003 101 MRDHIRNWLKEESGCQDADGGEEKWAMVYGMISPDMAEEKTMLKDLKTMLHSRMQMYAP----------
Brekke/98 101 MRDHIRNWLKEESGCQDADGGEEKWAMVYGMISPDMAEEKTMLKDLKTMLHSRMQMYALGASAKALETLEKAIVAAVHRLPASCSTEKMVLLGYLR
ISAV5(96/09/768) 101 MRDHIRNWLKEESGCQDADGGEEKWAMVYGMISPDMAEEKTMLKDLKTMLHSRMQMYALGASSKALETLEKAIVAAVHRLPASCSTEKMVLLGYLR
RPC/NB 04-085-1 101 MRDHIRNWLKEESGCQDAAGGEEKWAMVYGMISPDMAEEKTMLKDLKTMLHSRMQMYALGASSKALETLEKAIVAAVHRLPASCSTEKMVLLGYLR
ISAV8(97/09/615) 101 MRDHIRNWLKEESGCQDADGGEEKWAMVYGMISPDMAEEKTMLKDLKTMLHSRMQMYALGASSKALETLEKAIVAAVHRLPASCSTEKMVLLGYLR
Glesvaer/2/90 101 MRDHIRNWLKEESGCQDADGGEEKWAMVYGMISPDMAEEKTMLKDLKTMLHSRMQMYALGASSKALETLEKAIVAAVHRLPASCSTEKMVLLGYLR
901_09 101 MRDHIRNWLKEESGCQDADGGEEKWAMVYGMISPDMAEEKTMLKDLKTMLHSRMQMYALGASSKALETLEKAIVAAVHRLPASCSTEKMVLLGYLR

Figure S8

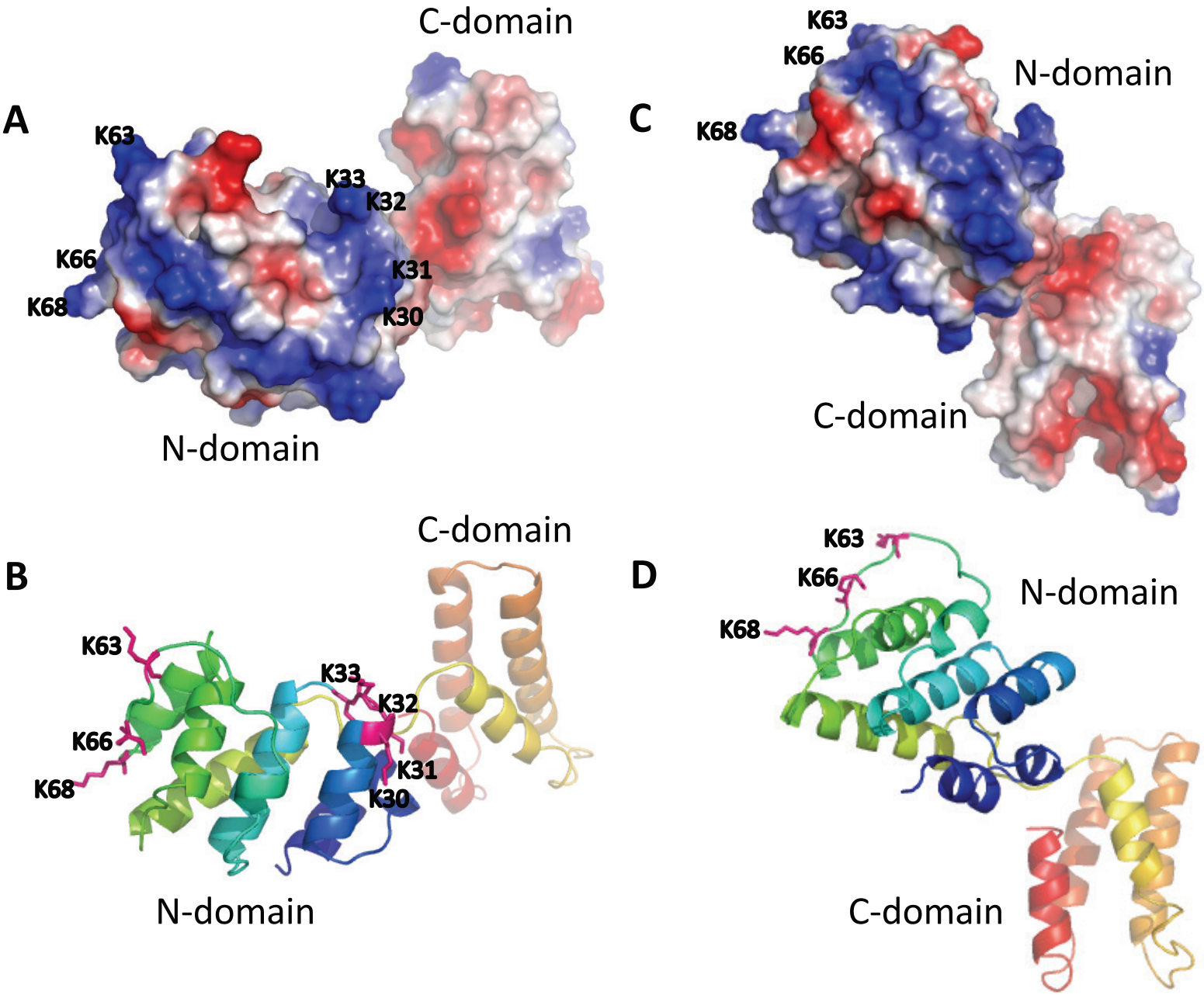
A
C-domain
K63
K33
K32
K66
K31
K68
K30
N-domain
C
K63
K66
N-domain
K68
C-domain
B
C-domain
K63
K33
K32
K66
K31
K68
K30
N-domain
D
K63
K66
N-domain
K68
C-domain

Figure S9

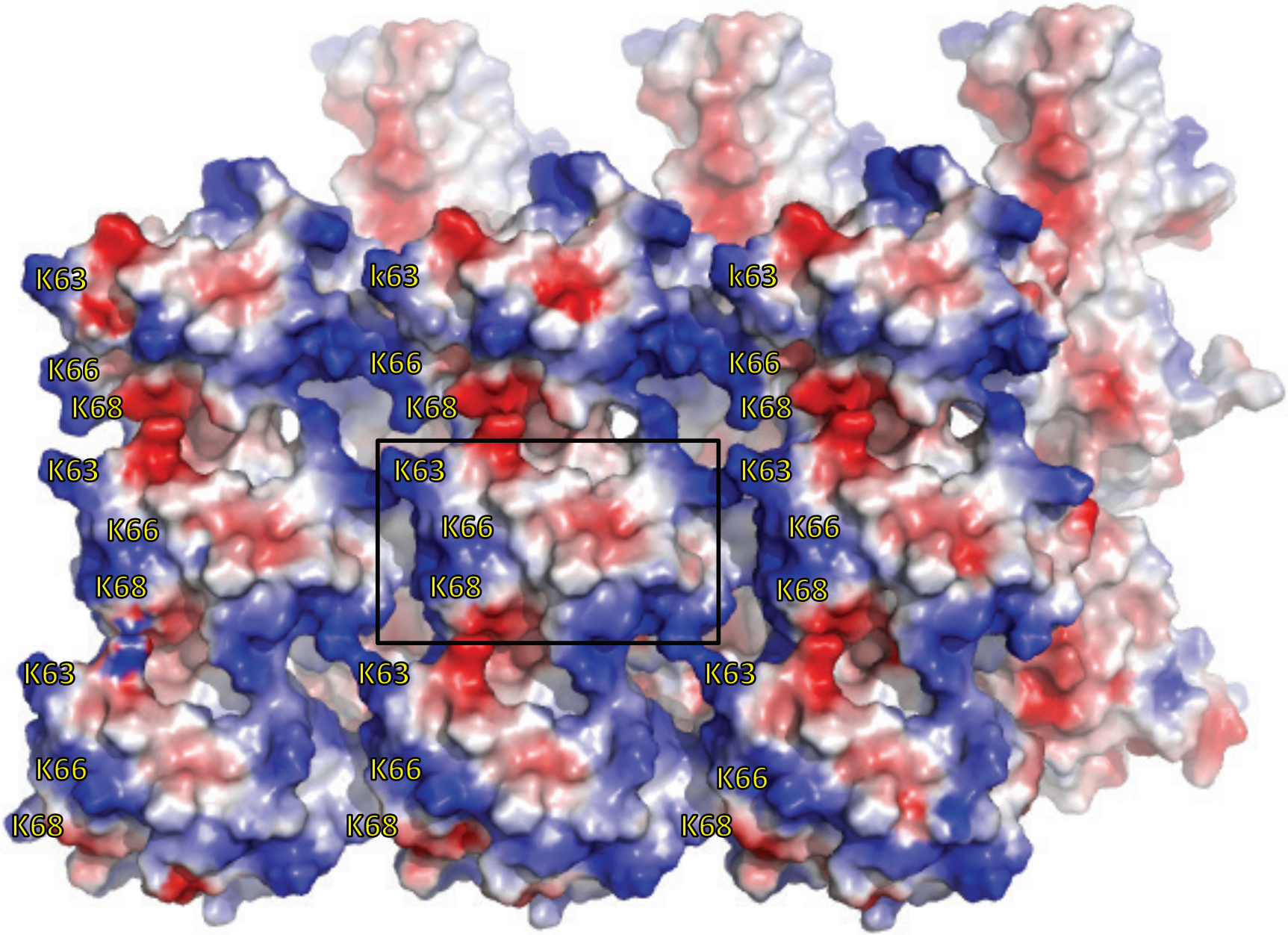
K63
k63
k63
K66
K66
K66
K68
K68
K68
K63
K63
K63
K66
K66
K66
K68
K68
K68
K63
K63
K63
K66
K66
K66
K68
K68
K68

Figure S10

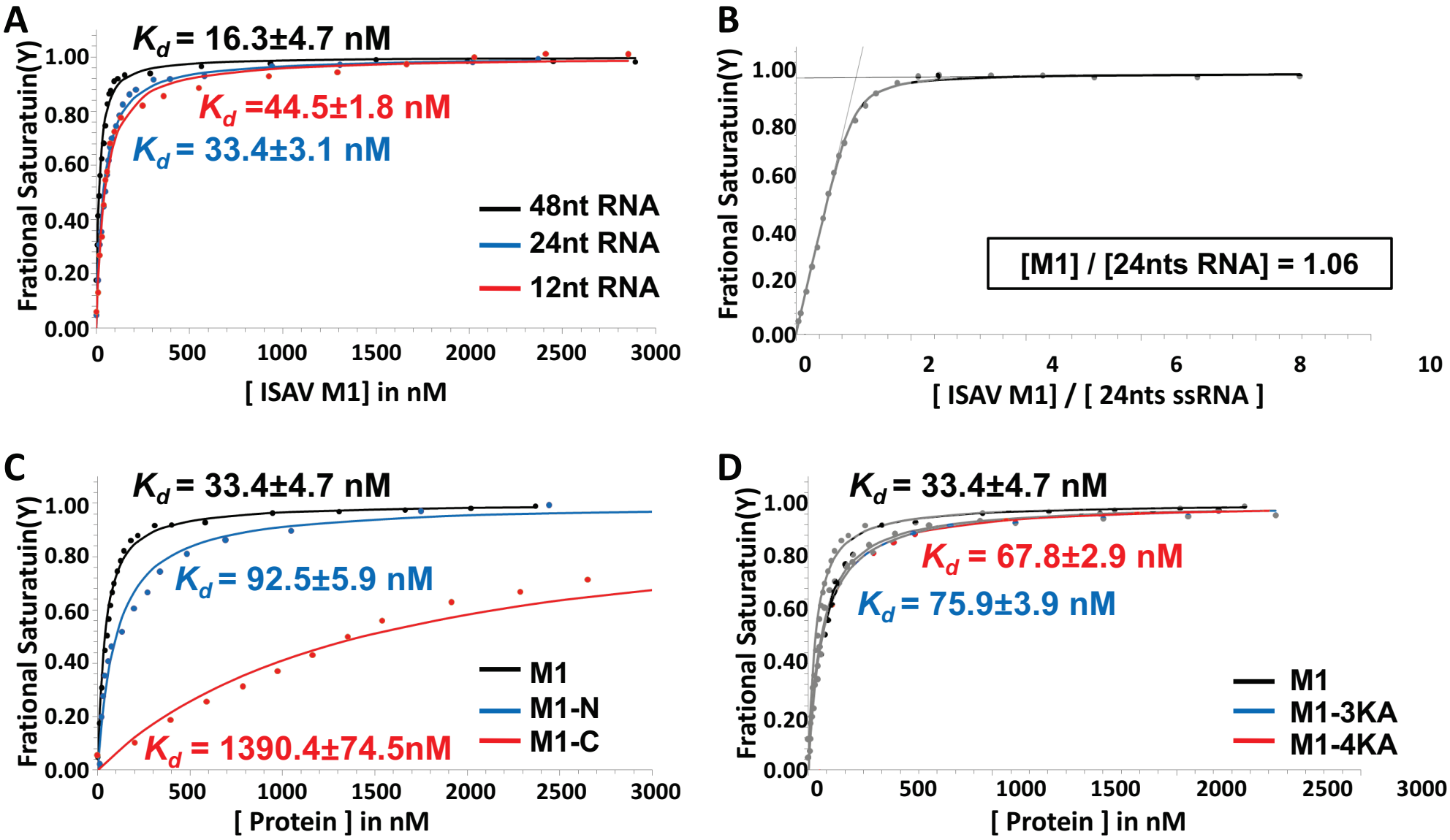
A
K_d = 16.3±4.7 nM
K_d =44.5±1.8 nM
K_d = 33.4±3.1 nM
48nt RNA
24nt RNA
12nt RNA
Frational Saturatuin(Y)
[ISAV M1] in nM
B
[M1] / [24nts RNA] = 1.06
Frational Saturatuin(Y)
[ISAV M1] / [24nts ssRNA]
C
K_d = 33.4±4.7 nM
K_d = 92.5±5.9 nM
K_d = 1390.4±74.5nM
M1
M1-N
M1-C
Frational Saturatuin(Y)
[Protein] in nM
D
K_d = 33.4±4.7 nM
K_d = 67.8±2.9 nM
K_d = 75.9±3.9 nM
M1
M1-3KA
M1-4KA
Frational Saturatuin(Y)
[Protein] in nM